Annals of the Academy of Romanian Scientists
Series on Engineering Sciences
ISSN 2066-8570 Volume **14**, Number **2**/**2022**

AERODYNAMIC STUDIES OF AIRCRAFT ENGINE TURBINE STAGE

Marcel ILIE[1], Augustin SEMENESCU[2]

Rezumat. *Studiile aerodinamice ale unei trepte stator-rotor pentru turbinele de motor de avion sunt efectuate computațional folosind metoda Large-Eddy Simulation (LES). Scopul acestui studiu este de a modela dinamica fluidului în această treaptă a motorului și în mod particular interacțiunea dintre palele rotorului și vârtejul format de stator. Calculele computaționale sunt efectuate pentru un regim variabil rotațional al rotorului. Studiul este efectuat pentru un număr Reynolds Re=1.3x10^5. Studiul prezent arată faptul că interacțiunea dintre vortexul format de stator și paleta rotorului produce o variație în timp a coeficienților specifici aerodinamici.*

Abstract. *The present research concerns the aerodynamic computational studies of stator-rotor turbine stage. The computational studies are carried out using the large-eddy simulation approach. In the aircraft engine compressor/turbine stage blade-vortex interactions occur. The present study aims at the understanding the blade-vortex interaction mechanism and its impact on the aerodynamics of rotor-stator compressor/turbine stages. The computational studies are carried out in a rotating frame of reference, for high-Reynolds number flow, Re = 1.3x10^5. The analysis reveals that the blade-vortex interaction causes the flow separation on the stator stage and a time-varying lift and drag.*

Keywords: numerical modeling, finite-differences, cavity flows

DOI https://doi.org/10.56082/annalsarscieng.2022.2.5

1. Introduction

Aircraft engines are complex thermodynamic systems that operate under a wide range of aerodynamic and thermal conditions, while these conditions define the propulsion efficiency of the engine. One of the challenges associated with the aircraft engines are the high-temperatures developed in the turbine stage. The high-temperature is due to the hot gases exiting from the combustion chamber, as schematically shown in Figure 1. The high-temperature affects the turbine blade

[1]PhD, Assistant Professor: Dept. of Mechanical Engineering, Georgia Southern University, Statesboro, GA 30458, USA, E-mail: milie@georgiasouthern.edu
[2]PhD, Professor, Dept. of Material Sciences, University Politehnica Bucharest, Bucharest, Romania,; Associate Member of Academy of Romanian Scientists. E-mail: augustin.semenescu@upb.ro

causing a rapid aging of the turbine blade. It is worth mentioning here that the turbine blades are exposed to the temperatures that exceed $1{,}600^0 C$. In the past decades, various methods were employed to mitigate the effects of these high temperatures. Therefore, novel materials withstanding high-temperatures were developed and tested. Ceramic materials were tested in the past and showed that they can withstand high-temperatures. However, these materials were too brittle and thus, they could not withstand the high vibrations encounter in the turbine stage. Therefore, alternative methods were tested for the mitigation of the high-temperatures. Therefore, one way of mitigating the effect of the high temperatures is to use the air cooling technique. The principle of the air-cooling technique is to inject low temperature air through fine orifices perforated through the blade as schematically shown in Figure 2.

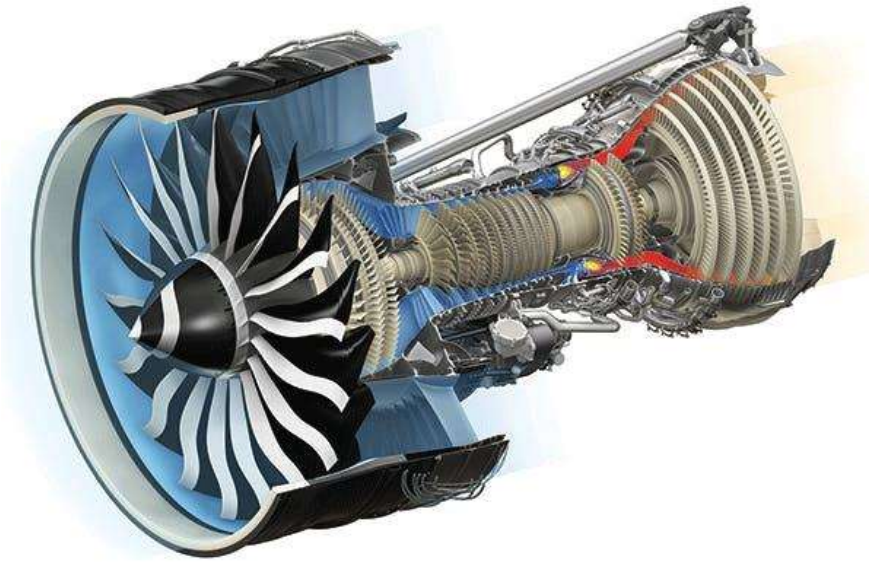

Fig. 1. Aircraft engine [20]

The fluid dynamics associated with the gas turbine engine blade is also complex and involves boundary-layer separation, blade-vortex interaction, and impinging-jet, as shown in Figure 4. Therefore, a good understanding of the fluid dynamics of the fluid flow associated with the turbine blade would improve the life span of the turbine blade and reduce the operational costs. Experimental studies of the fluid dynamics of turbine blade-cooling are challenging and costly and therefore, computational studies are more feasible and allow the repeatability of the experiment in a shorter time at minimum cost.

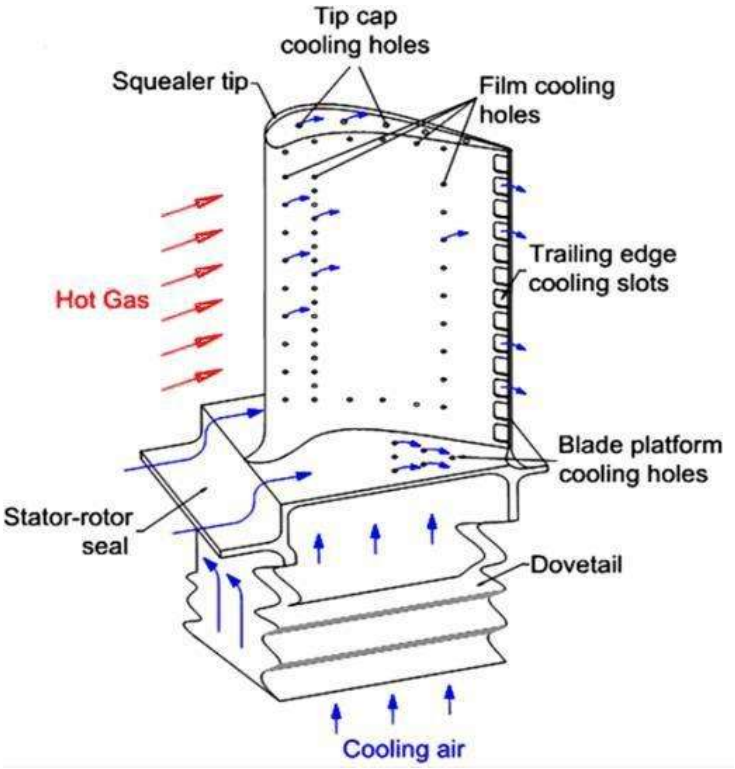

Fig. 2. Cavity flow for supersonic combustion [4]

Fig. 3. Cavity flow for supersonic combustion [19]

The present study concerns the feasibility of the air-cooling method for a stator-rotor-stator turbine stage as schematically illustrated on the Figure 3.

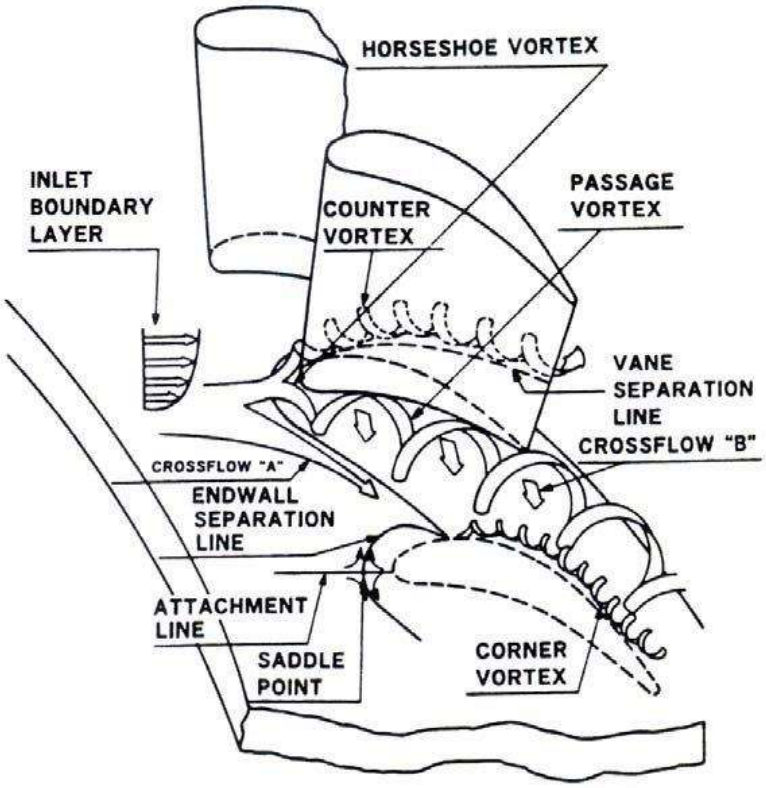

Fig. 4. Specific supersonic combustion cavity flow [18]

2. Background

Generally, the numerical computations of aerodynamics of turbine blades pose significant challenges due to the flow complexity and computational costs. [5, 7]. Studies showed that the numerical approach based on the "Reynolds-averaged Navier-Stokes (RANS) are not suitable for time-dependent flow dynamics such as the unsteady aerodynamics of compressor/turbine stage" [5]. Direct numerical simulations (DNS) also pose computational challenges due to the high-resolution grid size required by the DNS. Generally, DNS approach is not suitable for high Reynolds number flows and thus, alternative time-dependent solutions must be sought. Therefore, large-eddy simulation (LES) approach is a promising approach for the numerical computations of high-Reynolds number flows in a rotating-frame of reference.

3. Modeling and algorithms

As already mentioned in this research we will employ the LES approach. The specific equations using LES approach are the filtered Navier-Stokes equations (1) and (2)

$$\frac{\partial \bar{u}_i}{\partial x_i} = 0 \tag{1}$$

$$\frac{\partial \bar{u}_i}{\partial t} + \frac{\partial}{\partial x_j}\left(\bar{u}_i \bar{u}_j\right) = -\frac{\partial \bar{p}}{\partial x_i} - \frac{\partial \tau_{ij}}{\partial x_j} + \frac{1}{R_e}\frac{\partial^2 \bar{u}_i}{\partial x_j \partial_j} \tag{2}$$

where

$$\tau_{ij} = \overline{u_i u_j} - \bar{u}_i \bar{u}_j \tag{3}$$

The LES approach was used in the authors' previos studies [5]. "The SGS Reynolds stress, (τ_{ij}), is similar to the Reynolds stress in RANS in the sense that in both cases the unresolved scales (u') (small eddies in LES and turbulent fluctuations in RANS) are regarded as producing stresses in the resolved scales (large eddies in LES and mean velocity in RANS). The difference is that in RANS, (u') represents all the turbulent motions, while in LES (u') represents only the small eddies or sub-grid scales. This means that the energy in the unresolved scales of LES (sub-grid scales) represents a much smaller fraction of the total flow energy compared to the energy in the unresolved scales of RANS (the turbulent fluctuations)" [7].

Generally

$$\overline{u_i u_j} \neq \bar{u}_i \bar{u}_j \tag{4}$$

and therefore, Reynolds stress tensor (τ_{ij}) has to be modeled. The sub-grid scale (SGS) tensor τ_{ij} is expressed as:

$$\tau_{ij} - \frac{1}{3}\tau_{kk}\delta_{ij} = 2\nu\bar{S}_{ij} \tag{5}$$

where $\bar{S}_{ij}$ is the strain rate based on the filtered velocity $\bar{u}_i$ and the eddy-viscosity ν

$$\bar{S}_{ij} = \frac{1}{2}\left(\frac{\partial \bar{u}_i}{\partial x_j} + \frac{\partial \bar{u}_j}{\partial x_i}\right) \tag{6}$$

Smagorinsky model is an algebraic model for the subgrid scale (SGS) viscosity ν_{sgs}.

The space and time-discretization are presented in the following and were used in the authors' previous studies [5]. Figure 1 emphasizes the time and space-

marching schemes with space on the horizontal and time on the vertical. "For simplicity, an equally spaced computational domain will be used, with the space and time variables h and t. As shown in Figure 5, for the space marching of the solution, the time is fixed and solution is computed at the computational grid points $f(t,x-h)$, $f(t,x)$ and $f(t,x+h)$".

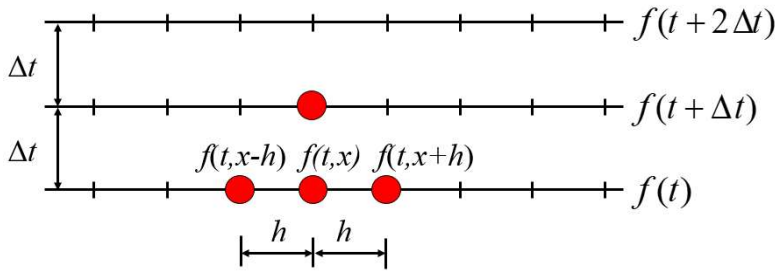

Fig. 5. Space and time-discretization

Figure 6 shows the time-discretization of the Laplace equation. For the time-marching, the space is kept constant while the time increment is $t+\Delta t$.

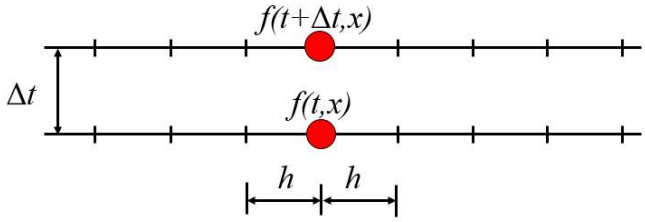

Fig. 6. Time-discretization

The finite-difference approach makes use of the Taylor series. Thus, the Taylor series is sued for an arbitrary function f, where f can represent the flow variables such as pressure or velocity [5]. The Taylor series expanded about the grid point $(x+h)$ becomes

$$f(x+h)=f(x)+\frac{\partial f(x)}{\partial x}h+\frac{\partial^2 f(x)}{\partial x^2}\frac{h^2}{2}+\frac{\partial^3 f(x)}{\partial x^3}\frac{h^3}{6}+\frac{\partial^4 f(x)}{\partial x^4}\frac{h^4}{24}+....$$

$$f(x-h)=f(x)-\frac{\partial f(x)}{\partial x}h+\frac{\partial^2 f(x)}{\partial x^2}\frac{h^2}{2}-\frac{\partial^3 f(x)}{\partial x^3}\frac{h^3}{6}+\frac{\partial^4 f(x)}{\partial x^4}\frac{h^4}{24}+....$$

Subtracting equation 3 from equation 2 and truncating the high-order terms, the difference $f(x+h)-f(x-h)$ is obtained such that

$$f(x+h)-f(x-h)=2\frac{\partial f(x)}{\partial x}h+2\frac{\partial^3 f(x)}{\partial x^3}\frac{h^3}{6}+....$$

Rearranging this equation to isolate the first derivative, we obtain the following equation:

$$\frac{\partial f(x)}{\partial x}=\frac{f(x+h)-f(x-h)}{2h}-\frac{\partial^3 f(x)}{\partial x^3}\frac{h^2}{6}$$

Next, we need to find the second derivative of function f. Making use again of the Taylor series

$$f(x+h)=f(x)+\frac{\partial f(x)}{\partial x}h+\frac{\partial^2 f(x)}{\partial x^2}\frac{h^2}{2}+\frac{\partial^3 f(x)}{\partial x^3}\frac{h^3}{6}+\frac{\partial^4 f(x)}{\partial x^4}\frac{h^4}{24}+....$$

$$f(x-h)=f(x)-\frac{\partial f(x)}{\partial x}h+\frac{\partial^2 f(x)}{\partial x^2}\frac{h^2}{2}-\frac{\partial^3 f(x)}{\partial x^3}\frac{h^3}{6}+\frac{\partial^4 f(x)}{\partial x^4}\frac{h^4}{24}+....$$

Adding equations, we obtain:

$$f(x+h)+f(x-h)=2f(x)+2\frac{\partial f^2(x)}{\partial x^2}\frac{h}{2}+2\frac{\partial^4 f(x)}{\partial x^4}\frac{h^4}{24}+....$$

Rewriting this equation in order to isolate the second derivative, is obtaining the second derivative of function f in the following structure:

$$\frac{\partial^2 f(x)}{\partial x^2}=\frac{f(x+h)-2f(x)+f(x-h)}{h^2}-\frac{\partial^4 f(x)}{\partial x^4}\frac{h^2}{12}+...$$

Canceling the high-order terms the second derivative equation is:

$$\frac{\partial^2 f(x)}{\partial x^2}=\frac{f(x+h)-2f(x)+f(x-h)}{h^2}$$

4. Results and interpretation

Figure 7 presents the velocity vector field for a stator-rotor-stator turbine stage. The analysis of the velocity field shows that there is an increase of velocity field from one stage to the other. An important result of the analysis is the presence of the trailing-edge vortices, at the stator-stage, which interact with the leading-edge of the rotor-stage. Moreover, the impinging cooled air jets causes an increase of the velocity at the leading-edge of the rotor stage blade row, as shown in Figure 7. These trailing-edge vortices interact with the rotor blade, mostly with the leading-edge of the rotor blade. The interaction between the trailing-edge vortices and rotor blades cause the blade-vortex interaction phenomenon. As the flow parcel passes the leading-edge of the rotor blade, a decrease of velocity is observed. The suction side of the stator blade experience a higher velocity as well as shown in Figure 7.

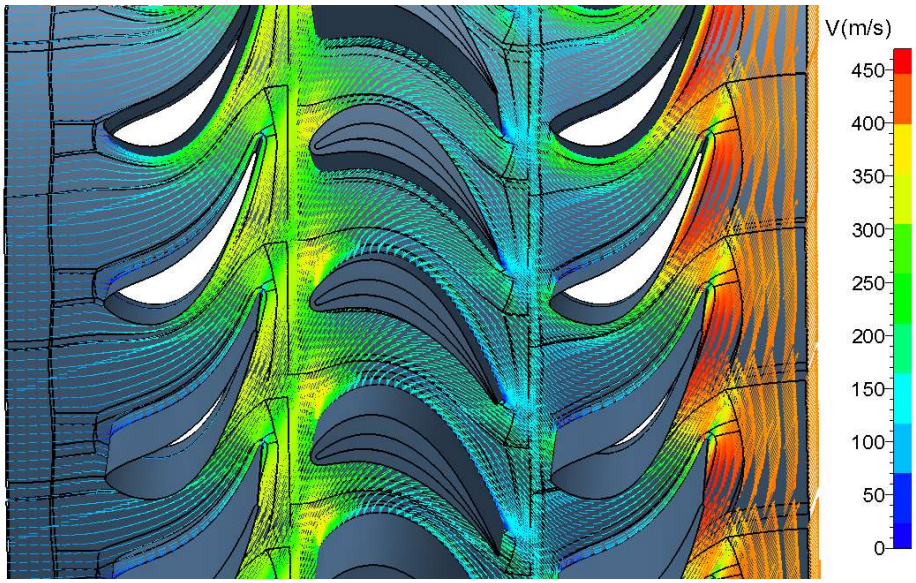

Fig. 7. Streamlines of the turbine stage

The analysis of the velocity vector field also reveals the presence of flow separation. The flow separation, at the leading-edge of the blade causes a decay of the aerodynamic performance of the turbine stage. Figure 8 presents the pressure field at the turbine stage. The analysis of the pressure field reveals a decrease of the pressure through the turbine stage. Figure 9 presents the temperature field through the turbine stage. Therefore, a pressure drop is seen across the first and second stator stages. A lower pressure is also seen on the suction side of the blade, at the first stator stage. The analysis of the temperature field shows the presence

of the cold air injectors and decreases the overall temperature in the turbine stage. Higher temperatures seen at the pressure side of the rotor blades and second stator stage. The study also reveals the high-temperatures at the leading- and trialing edges of the rotor stage. Figure 10 presents the vorticity field through the turbine stage. The analysis of the vorticity field reveals the presence of large vorticity levels on the suction side of the stator stages and this is due to the boundary-layer flow separation. therefore, vortices are formed at the suction side of the stator stages.

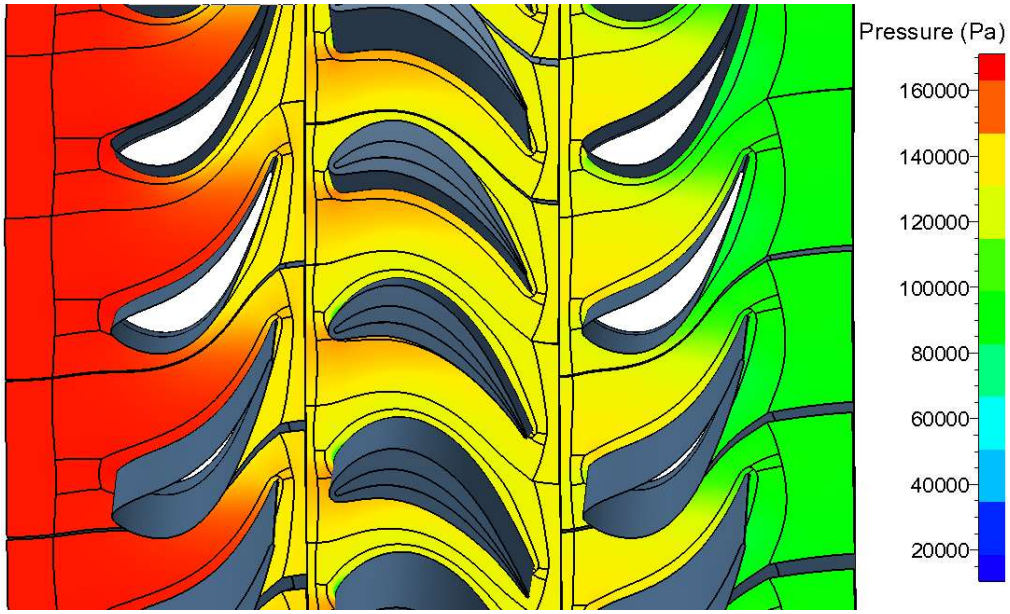

Fig. 8. Pressure field for the turbine stage

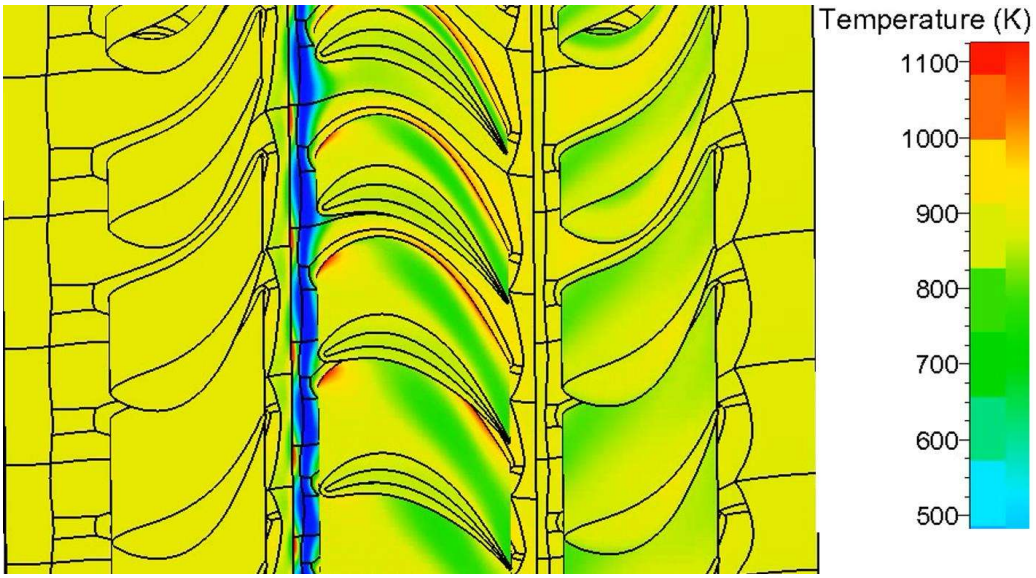

Fig. 9. Temperature field

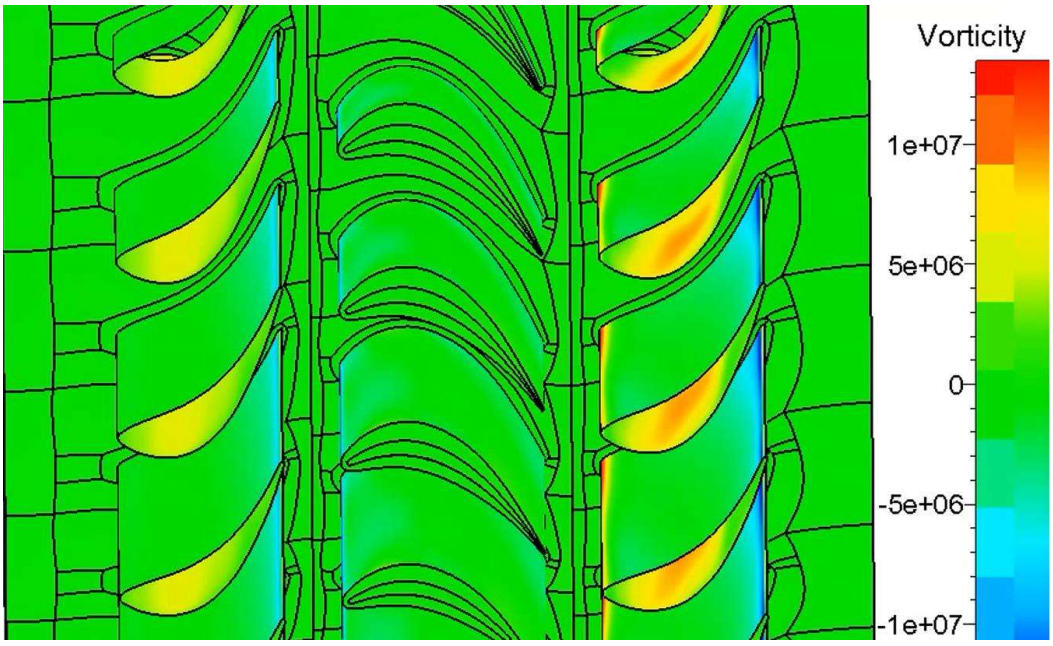

Fig.10. Vorticity field

Figure 11 presents the pressure fluctuations at locations downstream the turbine blade

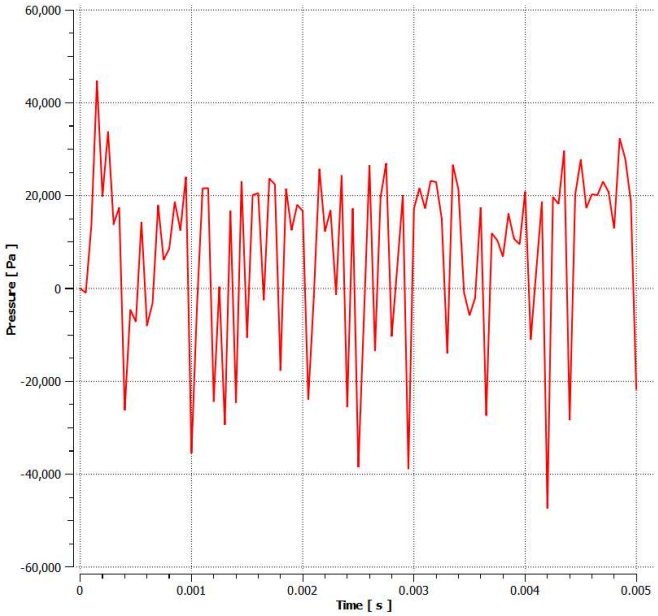

Fig. 11. Time-varying pressure

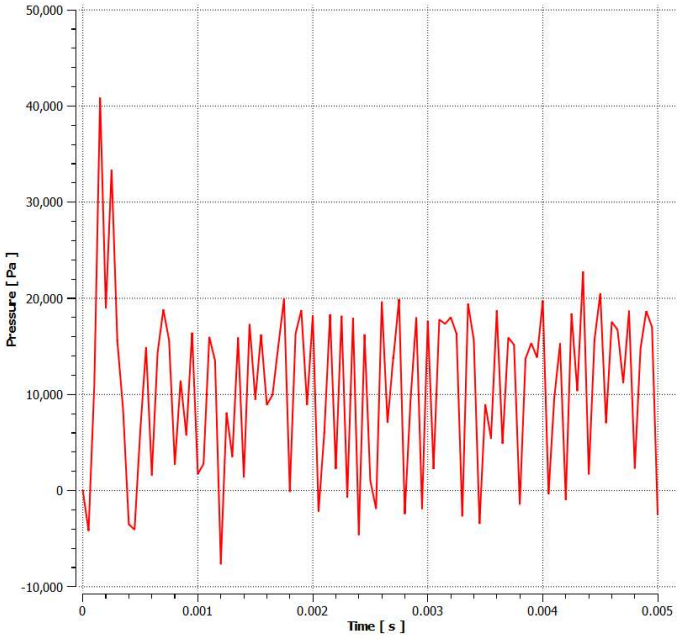

Fig. 12. Time-varying pressure

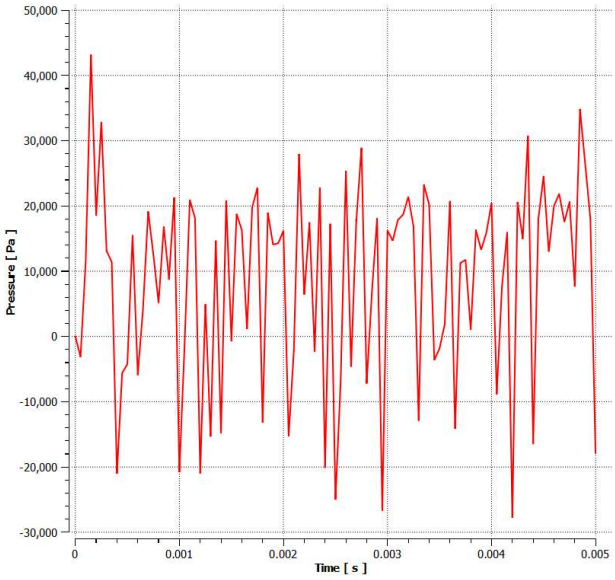

Fig. 13. Time-varying pressure

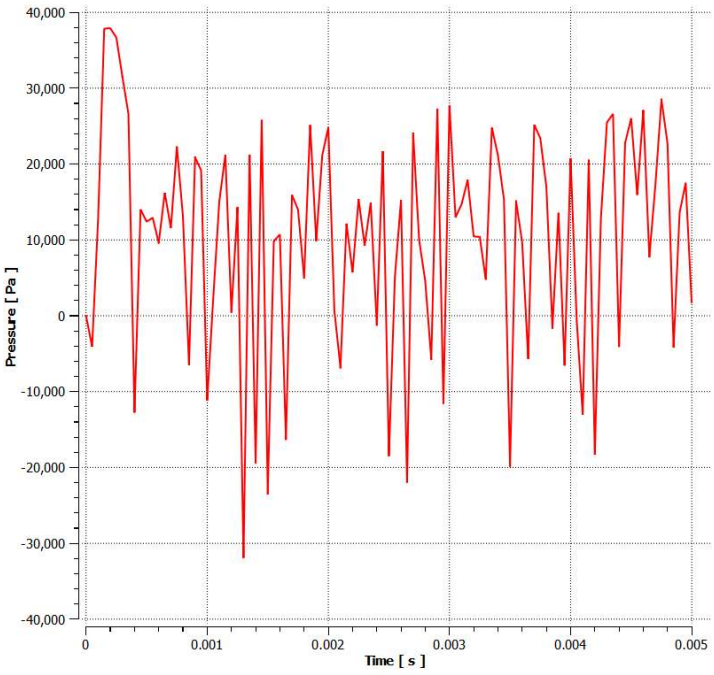

Fig. 14. Time-varying pressure

The analysis of the time-varying pressure reveals that there are large pressure fluctuations downstream the rotor blade and it is expected that these pressure fluctuations would affect the aerodynamic performance of the engine. The time-varying pressure is responsible for the flutter phenomenon in the turbine stage. Therefore, the aircraft engine performance is a tradeoff between the pressure and temperature or in other words between the fatigue and aging.

Conclusions

A computational model is developed for the aerodynamic computations of stator-rotor-stator stage in a rotating frame of reference. The analysis reveals that the computational domain capture very well the flow physics of the stator-rotor-stator stage. The study reveals that the air-cooling technique is an effective approach for the mitigation of the high-temperature through the turbine stage of the aircraft engine. The study reveals that there is a pressure drop across the turbine stage from first to second stator. High-temperature is observed on the suction side of the rotor-stage. The study also reveals the presence of a train of vortices at the trialing-edge of the stator blade which interacts with the rotor blade row. These interactions cause the flutter phenomenon in gas turbine engines.

REFERENCES

[1] E. Bilgen, H. Oztop, Natural convection heat transfer in partially open inclined square cavities, International Journal of Heat and Mass Transfer 48 (2005) 1470–1479, 2005

[3] D. Cherrared, Numerical simulation of film cooling a turbine blade through a row of holes, Journal of Thermal Engineering, Vol. 3, No. 2, 1110-1120, 2017

[4] K. Chang, G. Constantinescu, S.-O. Park, Journal of Fluid Mechanics 561, 113–145, 2006

[5] M. Ilie, A. Semenescu, G. Liliana Stroe, S. Berbente, Numerical Computations of the cavity flow using the potential flow theory, Annals of the Academy of Romanian Scientists Series on Engineering Sciences, Volume 13, Number 2/2021, ISSN 2066-8570

[6] M. Ilie. "A computational model for cardiovascular hemodynamics and protein transport phenomena", Health and Technology, 2021

[7] M. Ilie, Augustin Semenescu, Matthew Chan. "Computational studies of turbine- stage, with variable inlet temperature; comparison between LES and IDDES", AIAA AVIATION 2021 FORUM, 2021

[8] M. Ilie, Matthew Chan, Jackson Asiatico. "Combustion instabilities in backward-step premixed reacting flows; computational studies using LES", AIAA SCITECH 2022 Forum, 2022

[9] B.P. Leonard, A stable and accurate convective modeling procedure based on quadratic upstream interpolation, Computer Methods in Applied Mechanics and Engineering 19, 59–88, 1979

[10] J.C. Leong, N.M. Brown, F.C. Lai, Mixed convection from an open cavity in a horizontal channel, International Communications in Heat and Mass Transfer 32, 583–592, 2005

[11] O. Manca, S. Nardini, K. Khanafer, K. Vafai, Effect of heated wall position on mixed convection with an open cavity, Numerical Heat Transfer Part A 43, 259–282, 2003

[12] O. Manca, S. Nardini, K. Vafai, Experimental investigation of mixed convection in a channel with an open cavity, Experimental Heat Transfer 19, 53–68, 2006

[13] J. Pallares, I. Cuesta, F.X. Grau, F. Giralt, Natural convection in a cubical cavity heated from bellow at low Rayleigh numbers, International Journal of Heat and Mass Transfer 39, 3233–3247, 1996

[14] E. Papanicolaou, Y. Jaluria, Mixed convection from an isolated heat source in a rectangular enclosure, Numerical Heat Transfer, Part A: Applications 18, 427–461, 1990

[15] E. Papanicolaou, Y. Jaluria, Transition to a periodic regime in mixed convection in a square cavity, Journal of Fluid Mechanics 239, 489–509, 1992

[16] J.C.F. Pereira, J.M.M. Sousa, Experimental and numerical investigation of flow oscillations in a rectangular cavity, Journal of Fluids Engineering 115, 68–73, 1995

[17] Y. Stiriba, Analysis of the flow and heat transfer characteristics for assisting incompressible laminar flow past an open cavity, International Communications in Heat and Mass Transfer 35, 901–907,2008

[18] Takeishi, K., M. Matsuura, S. Aoki, and T. Sato (1990). An experimental study of heat transfer and film cooling on low aspect ratio turbine nozzles. J. of Turbomach. 112, 488—496.

[19] Gaetani, Paolo & Persico, Giacomo & Dossena, V. & Osnaghi, Carlo. (2007). Investigation of the Flow Field in a High-Pressure Turbine Stage for Two Stator-Rotor Axial Gaps—Part I: Three-Dimensional Time-Averaged Flow Field. Journal of Turbomachinery. 129. 10.1115/1.2472383.

[20] https://www.machinedesign.com/motors-drives/article/21832035/whats-the-difference-between-turbine-engines